

REVISED VERSION**ION IRRADIATION DAMAGE IN ILMENITE AT 100 K**

*J.N. Mitchell, N. Yu, R. Devanathan, K.E. Sickafus, and M.A. Nastasi,*  
Materials Science and Technology Division, Los Alamos National Laboratory,  
Los Alamos, NM 87545;

*G.L. Nord, Jr.,* United States Geological Survey, Reston, VA 22092

**ABSTRACT**

A natural single crystal of ilmenite ( $\text{FeTiO}_3$ ) was irradiated at 100 K with 200 keV  $\text{Ar}^{2+}$ . Rutherford backscattering spectroscopy and ion channeling with 2 MeV  $\text{He}^+$  ions were used to monitor damage accumulation in the surface region of the implanted crystal. At an irradiation fluence of  $1 \times 10^{15} \text{ Ar}^{2+} \text{ cm}^{-2}$ , considerable near-surface  $\text{He}^+$  ion dechanneling was observed, to the extent that ion yield from a portion of the aligned crystal spectrum reached the yield level of a random spectrum. This observation suggests that the near-surface region of the crystal was amorphized by the implantation. Cross-sectional transmission electron microscopy and electron diffraction on this sample confirmed the presence of a 150 nm thick amorphous layer. These results are compared to similar investigations on geikielite ( $\text{MgTiO}_3$ ) and spinel ( $\text{MgAl}_2\text{O}_4$ ) to explore factors that may influence radiation damage response in oxides.

**INTRODUCTION**

Spinel is exceptionally resistant to ion and neutron irradiation and, as a result, is being considered as an insulating material for fusion reactor applications [1-4]. Recently, Sickafus et al. [5] suggested that several characteristics may enhance radiation resistance in oxides: complexity of composition and the tendency for cation disorder. Clinard et al. [2] were the first to show evidence that compositional complexity enhances radiation resistance, and it does so by suppressing the nucleation and growth of dislocation loops and voids. Good examples of the defect characteristics of complex and simple compounds are spinel and  $\text{MgO}$ . In spinel, the formation of a dislocation loop requires the condensation of two or more  $\text{MgO} \cdot \text{Al}_2\text{O}_3$  anti-Schottky septets. Moreover, it is hard to condense point defects into loops because they are invariably faulted. Additionally, in spinel the

## **DISCLAIMER**

**This report was prepared as an account of work sponsored by an agency of the United States Government. Neither the United States Government nor any agency thereof, nor any of their employees, make any warranty, express or implied, or assumes any legal liability or responsibility for the accuracy, completeness, or usefulness of any information, apparatus, product, or process disclosed, or represents that its use would not infringe privately owned rights. Reference herein to any specific commercial product, process, or service by trade name, trademark, manufacturer, or otherwise does not necessarily constitute or imply its endorsement, recommendation, or favoring by the United States Government or any agency thereof. The views and opinions of authors expressed herein do not necessarily state or reflect those of the United States Government or any agency thereof.**

**DISCLAIMER**

**Portions of this document may be illegible  
in electronic image products. Images are  
produced from the best available original  
document.**

formation of anti-site defects occurs at much lower energies than either Frenkel or Schottky defects [6]. Thus, the major low energy defect structure is cation disorder. In MgO, however, it is much simpler to condense MgO molecular units and the lack of stacking faults makes loop nucleation easier. Also, these loops grow readily during irradiation, leading to a vacancy bias, void formation, and concomitant swelling [2].

To test the proposed radiation damage resistance criteria, we recently began an investigation of radiation damage response in ilmenite-group oxides. We chose this family of oxides because of their relative compositional complexity (two cations) and the tendency of  $\text{Fe}^{2+}$  and  $\text{Ti}^{4+}$  cations in ilmenite ( $\text{FeTiO}_3$ ) to disorder at high temperatures. In this paper, we describe the results of 200 keV  $\text{Ar}^{2+}$  irradiations of a natural ilmenite single crystal. Rutherford backscattering spectrometry combined with ion channeling (RBS/C) indicates that this material amorphizes at doses less than  $1 \times 10^{15} \text{ Ar}^{2+}/\text{cm}^2$ . Transmission electron microscopy (TEM) and electron diffraction confirmed this observation and revealed the presence of a 160 nm thick amorphous surface layer. The low ion irradiation tolerance of ilmenite suggests that chemical composition and crystal structure may be important in determining the radiation resistance of an oxide.

## BACKGROUND

The family of compositions we refer to as the ilmenite-group oxides are related by the fundamental composition  $\text{A}^{2+}\text{Ti}^{4+}\text{O}_3$ . In natural crystals, the divalent cation A can be Fe (ilmenite), Mg (geikielite), Mn (pyrophanite), or Zn (ecandrewsite), and there is substantial solid solution within this system. Crystals with Co, Cd, and Ni in the A site have also been synthesized. In nature, ilmenite is by far the most common of the rhombohedral titanates. Ilmenite is of interest as a potential substrate material for high  $T_c$  superconducting films [7], as a high-temperature, wide band gap semiconductor [8], and as a component of heavy concrete for radiation shielding in fission reactors [e.g., 9]. Ilmenite has been studied as a source for oxygen on proposed lunar bases [10], as a resource for  $\text{He}^{3+}$  for space fusion energy applications [11], and as a radiation-resistant semiconductor for satellites and related space applications [12].

Rhombohedral oxides such as ilmenite have crystal structures based on the hexagonal close-packing scheme. The cations sit on two-thirds of the available octahedral sites. The ilmenite structure is essentially an ordered version of the  $\alpha$ -alumina structure ( $R\bar{3}c$ ). The occupation of  $Fe^{2+}$  and  $Ti^{4+}$  instead of  $Al^{3+}$  doubles the number of crystallographically nonequivalent cation sites, reducing the space group symmetry to  $R\bar{3}$ . As shown in Fig. 1, Fe and Ti cations are layered along the [0001] direction. This ordering results in displacement of the anions away from the layers with larger cations toward the layers with the smaller cations.

The physical properties of ilmenite are closely linked to its solid solution relations with hematite ( $Fe_2O_3$ ). The properties of this solid solution series are the result of cation and magnetic order-disorder and low temperature immiscibility. The phase diagram (Fig. 2) of the system  $Fe_2O_3$ - $FeTiO_3$  has several important features: (1) a cation ordering transition; (2) a miscibility gap between disordered (hematite) and ordered (ilmenite) phases; and (3) a magnetic order-disorder transition. At room temperature, ilmenite with <27% hematite component is a p-type conductor, whereas if the hematite component is >27%, it is a n-type conductor [14]. The magnetic properties of ilmenite-hematite solid solutions range from paramagnetic to ferrimagnetic to antiferromagnetic [15, 16]. Except under extremely reducing conditions, natural ilmenite tends to have some component of  $Fe_2O_3$ . Ilmenite grains in volcanic rocks cool rapidly and  $Fe_2O_3$  remains dissolved in the quenched ilmenite. In rocks cooled over long periods of time, the hematite and ilmenite components will exsolve and form composite crystals, with the abundance of these phases controlled by bulk chemical composition. Lunar ilmenite has no hematite component due to the absence of  $Fe^{3+}$  on the Moon.

The crystal used for this study cooled slowly over millions of years and has approximately 20 volume % hematite that occurs as micron-scale ovoid exsolution structures. The cation order-disorder transition temperature for a crystal with this bulk composition is much higher than the temperature during our experiment (100 K). However, neutron- and ion-irradiated spinel crystals show greatly increased cation disordering at temperatures lower than capable of producing equiva-

lent thermally induced disorder [17, 18]. Thus, we anticipate that disordering in ilmenite may be similarly influenced by irradiation.

## EXPERIMENT

The sample used in this study is a natural single crystal of ilmenite collected in the Adirondack Mountains, New York. The crystal was oriented using Laue x-ray back reflection, cut into wafers perpendicular to the *c* axis, and polished to an optical finish on one side for ion-irradiation studies. Rutherford backscattering spectrometry combined with ion channeling (RBS/C) and ion irradiations were conducted at the Ion Beam Materials Laboratory at Los Alamos National Laboratory.

Two MeV He<sup>+</sup> ion beam RBS/C measurements were performed on the samples to verify the orientation of the crystal and to assess the quality of the polished surface. Aligned RBS spectra were obtained while the incident He<sup>+</sup> beam was aligned along the <0001> axis of the crystal. Minimum backscattering yield ( $\chi_{\min}$ ), defined as the RBS yield ratio of the aligned spectrum to that of the random spectrum, was used to quantify the quality of the sample surface. The initial high  $\chi_{\min}$  (~30%) indicated substantial residual damage in the near-surface region due to mechanical polishing. The damaged layer was effectively removed by etching the sample in a 50:50 mixture of hydrofluoric acid and water at room temperature for ~5 minutes, as indicated by the reduction in  $\chi_{\min}$  to ~6% along the *c*-axis.

Following etching, the crystal was irradiated at 100 K on a liquid nitrogen conduction-cooled sample stage. Ion-irradiation experiments were performed using 200 keV Ar<sup>2+</sup> at doses of  $1 \times 10^{15}$  and  $2 \times 10^{15}$  Ar<sup>2+</sup>/cm<sup>2</sup> on different portions of the crystal. The samples were tilted by 10° from the *c*-axis during the irradiations to minimize channeling effects. One section of the crystal was masked from the ion irradiation and used for ion channeling alignment following the irradiations. Unirradiated and irradiated regions of the crystal were analyzed with RBS/C along the <0001> axis using a 2 MeV He<sup>+</sup> ion beam. Random spectra were collected by rocking the sample about 3° off the <0001> channeling direction and are used for comparison with the aligned spectra.

The Monte Carlo code TRIM (Transport of Ions in Matter) [19] was used to estimate ion range and damage parameters (Fig. 3). TRIM simulations indicate that the projected range of 200 keV  $\text{Ar}^{2+}$  ions in ilmenite is 125 nm with a straggle of 42 nm. The peak concentration of Ar ions is 0.1 atomic % at a dose of  $1 \times 10^{15} \text{Ar}^{2+}/\text{cm}^2$ . At this dose, the peak damage level is  $\sim 1$  displacement per atom (dpa), assuming threshold energies of 20 eV for cations and 60 eV for anions.

Finally, the irradiated sample was prepared in cross section for transmission electron microscopy (TEM) observation to assess changes in microstructures induced by ion irradiation. Two portions of the section irradiated to a dose of  $1 \times 10^{15} \text{Ar}^{2+}/\text{cm}^2$  were glued face-to-face and then ground and polished to a thickness of  $\sim 20$  microns. The sample was further thinned by ion milling using 3-5 keV Ar ions. The finished sample was examined using a Philips CM30 TEM operating at 300 kV.

## RESULTS

RBS/C spectra of the three portions of the  $\langle 0001 \rangle$  aligned ilmenite crystal are shown with the random spectrum in Fig. 4. The spectrum from the unirradiated portion of the crystal is characterized by a low  $\chi_{\min}$  and very small Fe, Ti, and O surface peaks. The presence of hematite exsolution structures may have increased the dechanneling in this spectrum. The spectra acquired from sample regions irradiated to 1 and  $2 \times 10^{15} \text{Ar}^{2+}/\text{cm}^2$  are virtually identical, with the latter resulting in slightly higher RBS yields. The dechanneling yield from the irradiated layer at fluences of 1 and  $2 \times 10^{15} \text{Ar}^{2+}/\text{cm}^2$  coincide with the backscattering yield in a random-orientation spectrum. This is indicative of the formation of an amorphous layer in the irradiated region, or that the irradiated zone has become polycrystalline. The RBS/C results do not indicate the presence of defective crystalline material in the irradiated region, as has been observed in spinel [20, 21].

A more direct way to assess the nature of the damage in the irradiated region is by transmission electron microscopy of cross-sectioned samples. Using this technique, we observed in the sample portion irradiated with  $1 \times 10^{15} \text{Ar}^{2+}/\text{cm}^2$  a thin (150 nm) homogenous layer (Fig. 5a). Bend contours terminate at the interface between this layer and the substrate, indicating an abrupt transition

from a crystalline to amorphous material. Selected-area electron diffraction (SAED) patterns of this layer show diffuse rings around the transmitted beam, indicating that the layer is amorphous (Fig. 5b). In contrast, an SAED pattern of the substrate reveals the rhombohedral symmetry of ilmenite (Fig. 5c). No hematite was observed in the thin regions of the TEM foil, but its widespread presence in the bulk sample suggests that the lack of hematite in the foil is probably just by chance.

## DISCUSSION

Matzke [22] reported that ion-irradiated hematite became quasi-amorphous at a flux of  $2 \times 10^{16}$  ions/cm<sup>2</sup>, although the ion type, energy, and experimental temperature are not specified. Comparison between the experiment reported in this paper and those of Matzke [22] are difficult, but if hematite amorphizes more easily than ilmenite, the hematite grains present in our composite sample may act as amorphization nuclei and result in premature amorphization of the bulk crystal. However, the absence of hematite in the portion of the crystal that we studied with TEM suggests that ilmenite may have amorphized without the local influence of hematite. A more detailed investigation is needed to explore this potential relationship.

It is possible that the ion-irradiation process is not inert and that chemical reactions took place during the experiment [23]. Of particular concern is the possibility that redox reactions during irradiation may assist the precipitation of new phases, such as Fe<sub>3</sub>O<sub>4</sub>, Fe<sub>2</sub>O<sub>3</sub> and TiO<sub>2</sub>, resulting in a polycrystalline surface layer. RBS/C spectra taken from such a layer would be similar to those acquired from an amorphous surface layer. Korenevskii et al. [24] reported that iron in hematite was partially reduced to Fe<sup>2+</sup> during exposure to a fluence of  $1.3 \times 10^{20}$  neutrons/cm<sup>2</sup> at a temperature of 150 °C. Nevertheless, the electron diffraction pattern of the surface layer of the irradiated ilmenite in this experiment is consistent with an amorphous material, though we have not examined the valence state of iron in this region.

Our parallel investigation of radiation damage in geikielite (MgTiO<sub>3</sub>) indicates that it is considerably more radiation resistant than ilmenite under similar cryogenic irradiation conditions [23]. Geikielite and ilmenite are isostructural, differing only in composition. Similarly, pure fayalite



(Fe<sub>2</sub>SiO<sub>4</sub>) is less radiation resistant than fayalite-forsterite (Mg<sub>2</sub>SiO<sub>4</sub>) solid solutions [25]. Thus, chemical composition and insusceptibility to redox reactions may also play a role in determining ion radiation resistance.

The early stages of damage accumulation need to be examined to better discern the relationship between possible redox reactions and amorphization in composite ilmenite-hematite crystals. Also, ion-irradiation experiments on pure hematite would be useful to predict the behavior of hematite during irradiation of ilmenite-hematite intergrowths. In general, it does appear that ilmenite is easily amorphized by ion irradiation under low and ambient temperature conditions. However, we have recently demonstrated that ilmenite is not amorphized by 900 keV electron exposure [26], suggesting that it may be useful in environments where a semiconducting material that is resistant to light particle bombardment is needed.

## SUMMARY

We performed cryogenic ion-irradiation experiments on single-crystal ilmenite using 200 keV Ar<sup>2+</sup> to assess the radiation tolerance of ilmenite-group minerals. RBS/C and TEM indicate that the crystal amorphized easily compared to cryogenic irradiations of MgTiO<sub>3</sub> and MgAl<sub>2</sub>O<sub>4</sub>. These results suggest that numerous factors may influence the radiation response of an oxide, including chemical composition, propensity for cation disorder, insusceptibility to redox reactions, and crystal structure.

## ACKNOWLEDGMENTS

This research was funded by the U.S. Dept. of Energy, Office of Basic Energy Sciences, Division of Materials Sciences.

## REFERENCES

- [1] L.W. Hobbs and F.W. Clinard, Jr., J. Phys. 41 (1980) C6-232
- [2] F.W. Clinard, Jr., G.F. Hurley, and L.W. Hobbs, J. Nucl. Mater. 108/109 (1982) 655.

- [3] S.J. Zinkle, *J. Am. Ceram. Soc.* 72 (1989) 1343.
- [4] K. Nakai, K. Fukumoto, and C. Kinoshita, *J. Nucl. Mater.* 191-194 (1992) 630.
- [5] K.E. Sickafus, N. Yu, and M. Nastasi, *Nucl. Instru. Meth. B* 116 (1996) 85.
- [6] S.P. Chen, M. Yan, J.D. Gale, R.W. Grimes, R. Devanathan, K.E. Sickafus, N. Yu, M. Nastasi, *Phil. Mag. Lett.* 73 (1996) 51.
- [7] P.F. McDonald, A. Parasiris, R.K. Pandey, B.L. Gries, and W.P. Kirk, *J. Appl. Phys.* 69 (1991) 1104.
- [8] S.S. Sunkara and R.K. Pandey, *Cer. Trans.* 60 (1995) 83.
- [9] A.L. Brake, *Nuclear Energy Eng.* March (1959) 142
- [10] R.A. Briggs and A. Sacco, Jr., *Met. Trans. A* 24A (1993) 1257.
- [11] L.J. Wittenberg, J.F. Santarius, and G.L. Kulcinski, *Fus. Tech.* 10 (1986) 167.
- [12] R. Wilkins and R.K. Pandey, personal communication, 1996
- [13] G.L. Nord and C.A. Lawson, *J. Geophys. Res.* 97 (1992) 10987.
- [14] Y. Ishikawa, *J. Phys. Soc. Japan* 13 (1958) 37
- [15] S. Uyeda, *J. Geomagn. Geoelectr.* 7 (1957) 61.
- [16] Y. Ishikawa and S. Akimoto, *J. Phys. Soc. Japan* 12 (1957) 1083.
- [17] K.E. Sickafus, A.C. Larson, N. Yu, M. Nastasi, G.W. Hollenberg, F.A. Garner, and R.C. Bradt, *J. Nucl. Mater.* 219 (1995) 128.
- [18] E.A. Cooper, C.D. Hughes, W.L. Earl, K.E. Sickafus, G.W. Hollenberg, F.A. Garner, and R.C. Bradt, *Mat. Res. Soc. Symp. Proc.* 373 (1995) 413.
- [19] J.F. Ziegler, J.P. Biersack, and U. Littmark, *The Stopping and Range of Ions in Solids* (Pergamon, New York, 1985).
- [20] N. Yu, K.E. Sickafus, and M. Nastasi, *Phil. Mag. Lett.* 70 (1994) 235-240.
- [21] R. Devanathan, K.E. Sickafus, N. Yu, and M. Nastasi, *Phil. Mag. Lett.* 72 (1995) 155.
- [22] H.J. Matzke, *Can. J. Phys.* 46 (1968) 621.
- [23] J.N. Mitchell, N. Yu, K.E. Sickafus, M. Nastasi, T.N. Taylor, K.J. McClellan, and G.L. Nord, Jr., *Mat. Res. Soc. Sym. Proc.* 398 (1996) in press.

[24] V.V. Korenevskii, G.K. Krivokoneva, B.J. Pergamenschik, E.G. Ryabeva, and G.A. Sidorenko, *Inorg. Mater.* 7 (1971) 921.

[25] L.M. Wang and R.C. Ewing, *Mat. Res. Soc. Bull.* 17 (1992) 38.

[26] R. Devanathan, unpublished results (1996).

## FIGURE CAPTIONS

**Figure 1.** Ball and stick crystal structure model of ilmenite ( $R\bar{3}$ ). Other divalent cations that can substitute for Fe are Mg (geikielite), Mn (pyrophanite), Zn (ecandrewsite), Ni, Cd, and Co.

**Figure 2.** Phase diagram of the  $\text{Fe}_2\text{O}_3$ - $\text{FeTiO}_3$  system. Important features are the magnetic and cation order-disorder boundaries and the tricritical point. The crystal used in this study has approximately 80% ilmenite and 20% hematite. Figure adapted from Nord and Lawson [13].

**Figure 3.** Displacements per atom (dpa) and Ar concentration versus ion implantation depth, calculated using TRIM [19]. TRIM simulations indicate that the projected range of 200 keV  $\text{Ar}^{2+}$  ions in ilmenite is 124 nm and that the peak concentration of Ar ions is 0.1 atomic % at a dose of  $1 \times 10^{15} \text{Ar}^{2+} \text{ cm}^{-2}$ .

**Figure 4.** RBS/C spectra of irradiated and unirradiated portions of the ilmenite crystal used in this study. See text for discussion.

**Figure 5.** Bright-field transmission electron micrograph (a) of a cross section of the irradiated ilmenite crystal ( $1 \times 10^{15} \text{Ar}^{2+} \text{ cm}^{-2}$ ). The light region near the top of the photomicrograph is glue used to make the cross section. The underlying 160 nm thick layer is amorphous ilmenite, as revealed by the corresponding electron diffraction pattern in (b). Crystalline ilmenite underlies the amorphous layer, as indicated in (c).

Figure 1, Mitchell et al.

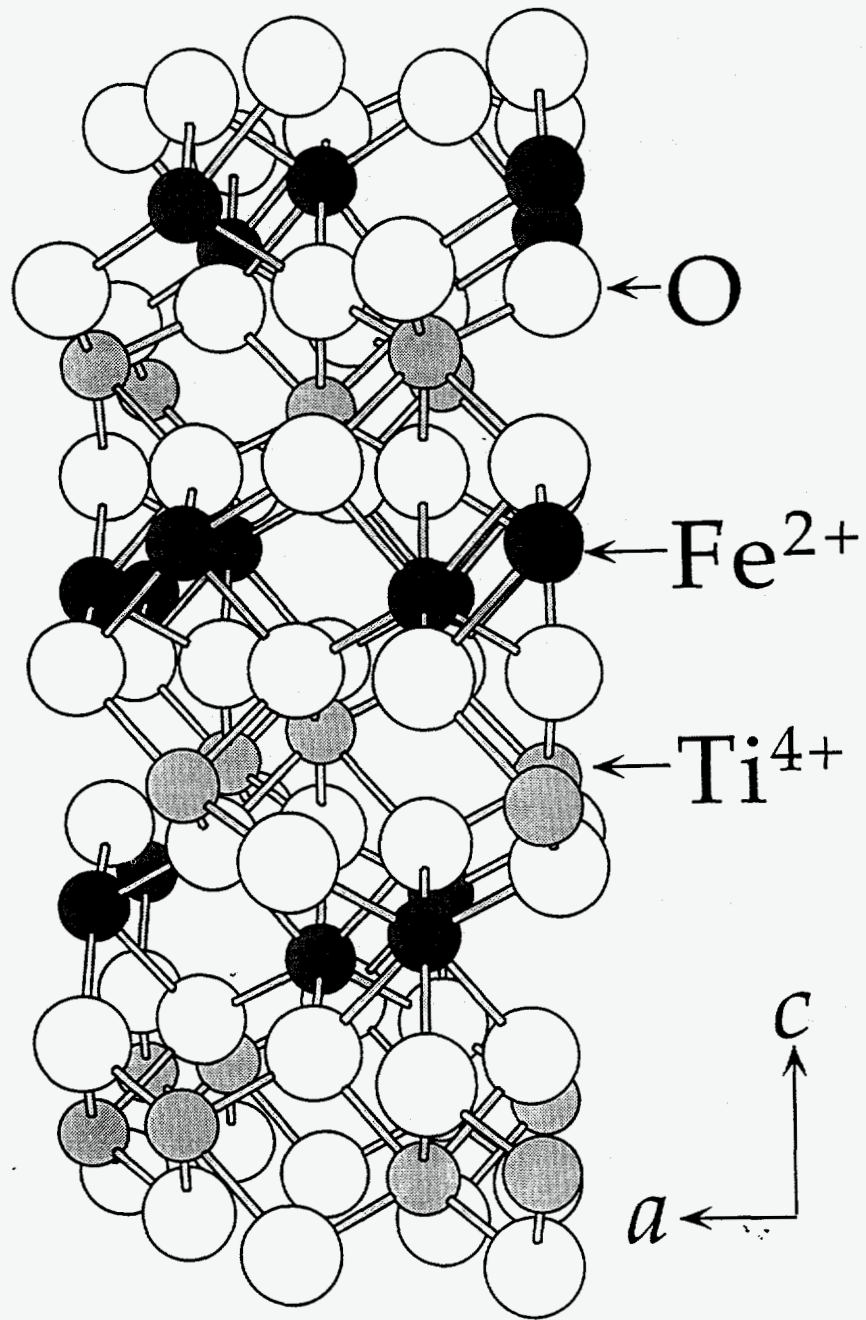


Figure 2, Mitchell et al.

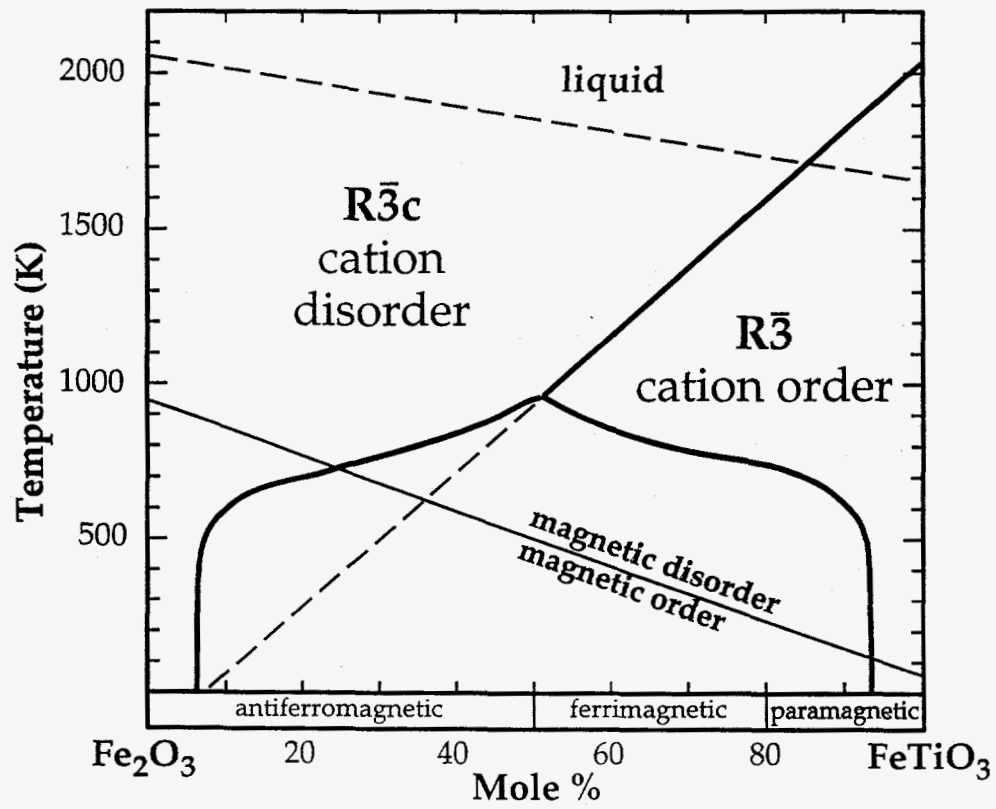


Figure 3, Mitchell et al.

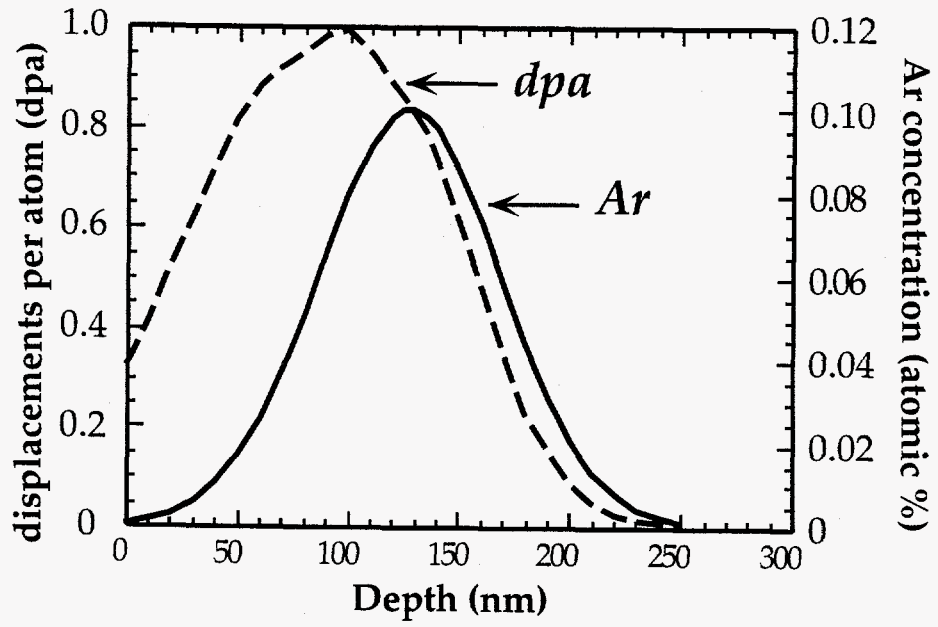


Figure 4, Mitchell et al.

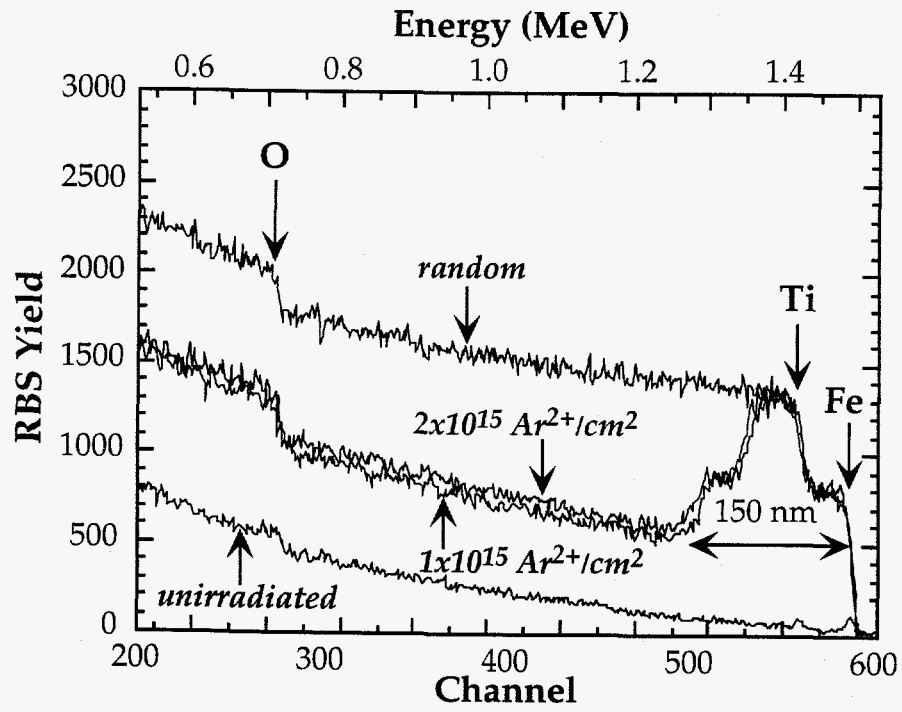


Figure 5, Mitchell et al.

